JOURNAL OF THERMOPHYSICS AND HEAT TRANSFER
Vol. 10, No. 2, April–June 1996

Spectral–Directional Emittance of Oxidized Copper

Peter D. Jones,* Devadas E. Dorai-Raj,† and David G. McLeod‡
Auburn University, Auburn, Alabama 36849-5341

The surface emittance of fully oxidized copper is experimentally determined as functions of wavelength between 2–10 μm, the direction between the normal and grazing angles, and the temperature between 400–700°C. Clean copper surfaces, heated and exposed to air, begin to oxidize immediately. After a sufficient heating time, the oxide layer becomes thick enough that the radiative surface properties are those of copper oxide, independent of the properties of the underlying copper. The experimental apparatus measures emitted flux over discrete bands of wavelength and solid angles centered about a direction, and is calibrated with a radiating cavity (hohlraum). Emittance results are presented in both spectral and polar form, and also integrated to obtain the spectral–hemispherical emittance of fully oxidized copper. By assuming copper oxide to be a dielectric, the real part of the index of refraction is reduced from emittance data. This index is found to decrease with wavelength and temperature. This technique of spectral–directional emittance determination by direct emission measurement, together with index of diffraction identification (if found to fit Fresnel or other relations), should prove useful for other engineering materials as well as copper oxide.

Nomenclature

a = side dimension of square test article surface, m
C = calibration factor for radiometer reading
g = acceleration of gravity, 9.81 m/s^2
$I_{\lambda b}$ = spectral blackbody intensity, W/(m^2-μm-sr)
k = thermal conductivity, W/m-K
k_λ = spectral imaginary index of refraction
Nu = Nusselt number
n_λ = spectral real index of refraction
R = radiometer reading, W/m^2
S = sample standard deviation
T = temperature, K
t = material thickness, m
$t_{2,90}$ = student-t parameter, 2 degrees of freedom, 90% confidence $\therefore$ = 2.920
u = uncertainty, units of subscript
α = thermal diffusivity, m^2/s
$\delta\lambda$ = monochromator wavelength interval, μm
$\delta\Omega$ = optical path acceptance solid angle, sr
ε = emittance
θ = surface polar angle, rad
λ = wavelength, μm
ν = kinematic viscosity, m^2/s
σ_b = Stefan–Boltzmann constant, 5.67 × 10^{-8} W/m^2-K^4

Subscripts
a = air over test article surface
Cu = copper
c = calibration blackbody
co = copper oxide
s = test article surface
ss = test article subsurface
∞ = surroundings visible to test article surface

Received March 6, 1995; revision received July 25, 1995; accepted for publication Dec. 14, 1995.

*Assistant Professor, Mechanical Engineering Department. Member AIAA.

†Graduate Student, Mechanical Engineering Department; currently Engineer, J. H. Kelly Co., 1550 East, 3400 North, Suite 300, Lehi, UT 84043.

‡Graduate Student, Mechanical Engineering Department; currently Engineer, Lexmark International, Inc., 740 New Circle Road, Lexington, KY 40511.

Introduction

HOT copper surfaces, when exposed to air, immediately oxidize and a covering layer of copper oxide begins to grow. Copper blocks are often used in heat transfer research apparatus because of the high thermal conductivity of copper, making constant temperature conditions easier to approximate. Therefore, it is important to know the emittance of naturally oxidized copper to evaluate radiative heat transfer effects in such apparatus. Many of the radiative heat transfer numerical modeling techniques that are coming into widespread application (Monte Carlo, discrete ordinates, etc.), easily accept surface boundary emittances that vary with wavelength and direction. Therefore, availability of spectral–directional emittance data allows more detailed computation of radiative transfer effects than is possible using total and/or hemispherical properties.

Most of the data available in the literature for copper oxide present the variation of the total-normal and total-hemispherical emittance with temperature.[1–12] Many of these studies use outdated equipment, and test surface preparation is often not well defined. There is remarkably little agreement on the magnitude of the emittance between literature sources, or on its relation to temperature. Total emittance cannot be derived from the present work because of spectral range limitations in the detection apparatus. Extension of this work to measure total emittance would be helpful in resolving these disagreements.

There is some data on the spectral–normal[5,13] emittance of copper oxide in the literature, although these data are sparse and too scattered to make functional correlations over the whole spectral range of thermal radiation. There are no data in the literature on the spectral–directional emittance of copper oxide.

The purpose of the present study is to determine the spectral–directional emittance of naturally oxidized copper to provide boundary conditions for radiative transfer computational techniques that are sensitive to data in this form. The directional range covered by this study excludes very nearly grazing angles because of the size of the apparatus acceptance cone. The spectral range is limited to between 2–10 μm, and the temperature range is limited to between 400–700°C by the constraints of the present apparatus. Further study with more capable equipment is recommended.

Apparatus

Surface emittance is determined using an apparatus for the measurement of radiative flux within a finite cell of solid angle

and a band of wavelength (shown in Fig. 1). For small solid angles and bands, this flux is taken as the radiation intensity. A cone of radiation leaving a surface (1 on Fig. 1) is reflected from an off-axis parabolic segment reflector (6; gold plated), resulting in a collimated beam. The beam is trimmed by reflecting away all but the 19-mm-diam center portion (8), and the remaining beam is chopped to allow comparative (open path to closed path) noise filtering (9). The beam is transmitted through one of a battery of optical edge filters (10), and is refocused by a second off-axis parabolic reflector (11; identical to 6) into a one-eighth-m grating monochromator (12) to achieve spectral discrimination. Filtering is necessary as the monochromator accepts $\lambda/2$, $\lambda/3$, $\lambda/4$, etc., as readily as λ, and these higher-order terms must be removed. Optical path alignment is achieved using a pair of visible diode lasers, mounted in a jig to hold them parallel and at opposite edges of the path. The output of the monochromator (12) is focused onto a pyroelectric detector (13; electrically polarized lithium tantalate crystalline chip), whose output is amplified and taken to a radiometer control unit (14). The control unit (14) compares the detector (13) signal rise during the open chopper interval (signal plus noise) to that during the closed chopper interval (noise), and displays a voltage proportional to the radiant power incident on the detector through the optical path. The acceptance solid angle of the intensity measurement system optical path is 0.020 sr (maximum polar variation 9 deg), while the monochromator passes a wavelength band that varies between 0.026 μm in width at a wavelength of 1.5 and 0.16 μm in width at 10 μm. The radiometer display is taken as proportional to the radiative intensity, averaged over this solid angle and wavelength band. Calibration is performed over the same set of solid angles and wavelength bands as those over which the measured data is taken. Polarization effects for radiation emitted by the rough oxidized surface are neglected, although the test article was rotated to ensure that there was no bias because of orientation.

The intensity measurement system is intended to measure the moderately diffuse, randomly polarized, broadband intensity issuing from the surfaces of hot objects, and is calibrated using a blackbody source (5). The source cavity consists of a 63.5-mm-diam cylinder, 152 mm deep with a 45-deg conical end, bored into 152-mm-diam high-grade (99.9% purity) copper stock. The cavity is closed with a 25-mm-thick copper faceplate, through which the 9.5-mm aperture is bored [the aperture is the small end of a truncated 15-deg cone, so that direct emissions from the sides of the aperture cone are not passed into the field of view (FOV)]. The blackbody is packed in a 75-mm layer of a ceramic wool insulating blanket. Eight cartridge heaters and a J-type thermocouple embedded in the cavity wall employ an autotuning control with a 10-s time constant to maintain the thermocouple temperature within (−1°C, +0) of the set point. A numerical model of transient conductive and radiative transfer within and between the blackbody walls shows a maximum deviation of 1°C between the control thermocouple and any point on the cavity surface. Blackbody temperatures up to 700°C may be maintained. Since the blackbody aperture is of finite size, the intensity exiting the aperture is less than the blackbody intensity, and depends on the emittance of the cavity walls. The blackbody was operated continuously for several hundred hours to ensure growth of a thick crust of copper oxide on its surfaces. A diffuse-gray 30-element surface radiation analysis of the cavity using blackbody radiation at ambient temperatures for the incoming radiosity of the aperture and using a total-hemispherical emittance for copper oxide of 0.73 shows that the effective aperture emittance is roughly 0.999. The collecting off-axis parabolic reflector (6) may be rotated (7) so that the detector will sense either the blackbody or the test surface radiation.

The collecting reflector (6) may be rotated to view the test surface (1) from angles at 6-deg increments between 0–84 deg, as shown in Fig. 2. The test surface (1) is mounted in a test article holder (2), which hangs on trunnions (3) that may be moved into different slots on a 90-deg arc circular rack (4). As the collecting reflector (6) is rotated (7), its focal point is held to the same spot on the test article surface. This combination of movements allows radiative flux within a 0.020-sr cell of solid angle to be measured at angles relative to the surface of the test article, allowing a full variation in surface-relative polar angle. The test article (1) is attached to the top of a heater block comprised of a 75-mm cube of copper with two cartridge heaters and two thermocouples embedded in it. One thermocouple protrudes into the test article, though not to its surface. The second thermocouple is located near the heaters. The test article temperature controls the heater block in a manner similar to the blackbody source. The test article/heater block assembly is open to the surroundings on its top (measurement) face, and is otherwise packed in a ceramic wool insulation blanket enclosed by a casing (2). The trunnions (3) are attached to the test article holder casing.

The test article is a 75 mm square of industrial high grade (99.9% purity) copper, 6 mm thick. It is milled to a no. 8 lathe

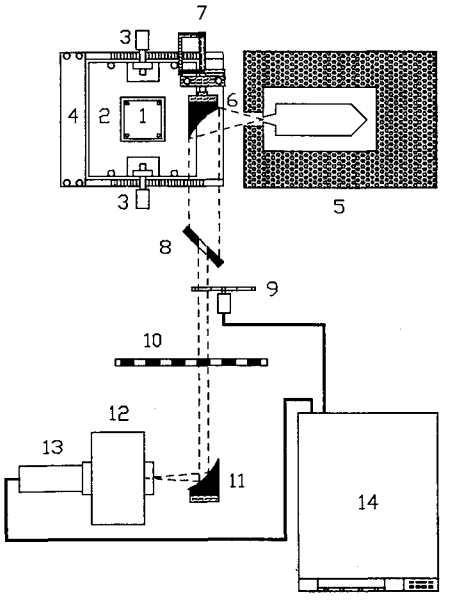

Fig. 1 Radiation intensity measurement system: plan view. System components: (1) test surface/test article, (2) test article holder, (3) trunnions, (4) slotted arc rack, (5) blackbody, (6) collecting reflector, (7) reflector rotation mechanism, (8) trimming plate, (9) chopper, (10) filter rack, (11) refocussing reflector, (12) monochromator, (13) detector, and (14) radiometer control unit.

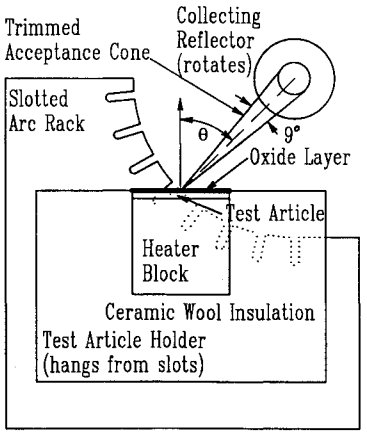

Fig. 2 Arrangement for varying intensity measurement direction relative to the surface normal: elevation viewed from axis of optical path.

finish (polished smooth, but not mirror-like, with small scratches and imperfections plainly visible), and thoroughly cleaned to remove foreign films and particles.

Apparatus have been prepared by Heinisch,[14] Hesketh,[15] and Brandenberg[16] that are similar in various features to the present apparatus, and these were used in emittance measurements, respectively, for stainless steel, microgrooved silicon, and platinum mirrors, grooved surfaces, and black paint.

Procedure

The copper surface discolors quickly at elevated temperatures, and a film of copper oxide is observed to grow. Copper oxide has both a higher emittance and a lower thermal conductivity than copper. Therefore, asymptotic levels in transient measurement series of subsurface temperature and emitted intensity may be used to identify an asymptotic oxide thickness. A period of 300 h was found to be sufficient to allow all transients to die out (during which the subsurface temperature was between 400–700°C). Data were taken over the next 200 h over full ranges of wavelength, direction, temperature, test surface orientation (azimuthal rotation), and measurement spot location (displacement). Repeatability to within the experimental uncertainty (following) was found for all parameter variations. After 500 h of heating, an oxide film thickness of 0.40 mm was measured (±0.05 mm; slightly rough in appearance).

X-ray diffraction analysis of a 0.4-mm-thick oxide chip from the surface of the test article indicated interference peaks that correspond with the major peaks of CuO. An additional peak was also present that corresponds with Cu_2O, although none of the other Cu_2O peaks were detected. As CuO has a lower formation energy than Cu_2O, it might be expected that the oxide layer would be composed of CuO. However, it is possible that in a thick oxide layer, oxygen starvation results in Cu_2O formation at the copper surface, while CuO is formed in the initial growth of the oxide and dominates the oxide surface. Therefore, it appears that the present data primarily address CuO, although the presence of some other compound, possibly Cu_2O, was detected.

To not interrupt the copper oxide surface, the surface temperature measurement thermocouple was embedded in the test article to a point slightly beneath the surface of the copper. Heat flux through this thin layer of copper and through the copper oxide film (which has a low thermal conductivity), was compared to the heat flux from the test article surface (determined using free convection heat transfer correlations and the total-hemispherical emittance of copper oxide) to estimate the actual surface temperature. Since the oxide thickness cannot be accurately measured until after completion of all measurements, the test article surface temperature cannot be known at the time of measurement, and the blackbody source cannot be set to this temperature for on-line calibration. Instead, the intensity measurement system was calibrated in advance using the blackbody, measuring the correlation of measurement signal to blackbody intensity as a function of temperature and wavelength. Repeated measurements of this correlation demonstrated an uncertainty less than or equal to 2% (except for $T_s < 400$°C, $\lambda < 3$ μm, or $\lambda > 10$ μm, where lower emissive power levels drive uncertainty to 3%).

Test surface emittance was determined by comparing the measured intensity leaving the test article surface with the calibrated blackbody intensity of the test article surface temperatures. The influence of reflected intensity was reduced by minimizing the presence of hot objects within the test surface FOV, as shown in Fig. 2. All parts of the test article holder assembly were at or beneath the plane of the test article surface. The blackbody source was switched off and allowed to cool prior to test article intensity measurements. All components of the circular arc rack and optical train are no hotter than slightly warm to the touch (~40°C; recall that data are taken for test article temperatures of 400°C and above). The 1.1-m total optical path is long enough that it is difficult for stray radiation to pass through all of the apertures. Reflection from the detector surface back through the optical path has a negligible effect on the data because of transmission losses in the filters, low reflectance of the lithium tantalate detector, and diffuse rather than specular reflection from the detector surface.

Following an oxide film growth period, spectral series (18 wavelength points) were measured at each polar angle (eight directional points). After reaching the 300-h oxidation time, the temperature of the test article was successively reduced from 700°C in 100-deg steps to complete the measurement matrix. Higher temperatures were occasionally returned to ensure repeatability. No repeatability difficulties were found once the film growth period was complete. Copper oxide is a brittle material that cracks and flakes off when the test article is cooled to room temperature. Therefore, the test article was kept above 400°C continuously until all measurements were complete. To test for sample bias, a second test article was prepared and a limited range of data was taken. Variations between the first and second test articles are within the experimental uncertainty.

Data Reduction

A calibration factor is determined as

$$C(\lambda, T_c) = \frac{1}{R_c(\lambda, T_c)} \left[\int_{\lambda-\delta\lambda/2}^{\lambda+\delta\lambda/2} I_{\lambda b}(T_c)\, d\lambda \right] \delta\Omega \qquad (1)$$

where R_c is the radiometer measurement taken with the blackbody source set at T_c and the filters and monochromator set for λ. The measurement R_c is a function of the blackbody radiation and the various reflectivities and transmissivities, monochromator aperture and cone corrections, grating efficiency, and detector area, as explored more thoroughly by Dorai-Raj.[17] The factor C is found to have a very weak dependence on T_c (within the experimental uncertainty over the measurement range), indicating that the intensity measurement system may be regarded as linear. The spectral–directional emittance is determined by

$$\varepsilon_{\lambda,\theta}(T_s) = \frac{R_e(\lambda, \theta, T_s) C(\lambda, T_s)}{\left[\int_{\lambda-\delta\lambda/2}^{\lambda+\delta\lambda/2} I_{\lambda b}(T_s)\, d\lambda \right] \delta\Omega} \qquad (2)$$

where R_e is the radiometer measurement taken from the test surface, and T_s is the calculated test surface temperature, determined after the test article has cooled and the thickness of the flaked-off copper oxide has been measured. The measurement solid angle $\delta\Omega$ about θ and the measurement wavelength band $\delta\lambda$ about λ are constant between R_c and R_e. The data reduction system of Eqs. (1) and (2) would amount to simply the ratio of R_e to R_c, except that T_s differs slightly from T_c.

The surface temperature is resolved from

$$\frac{T_{ss} - T_s}{(t/k)_{Cu} + (t/k)_{co}} = Nu \frac{4k_a}{a} (T_s - T_a) + \varepsilon\sigma_b(T_s^4 - T_\infty^4) \qquad (3)$$

where the correlation

$$Nu = 0.54 \left[\frac{ga^3}{32(T_s + T_a)\nu_a\alpha_a} (T_s - T_a) \right]^{1/4} \qquad (4)$$

corresponds to a hot, horizontal square surface facing up.[18] Published data[18,19] are used for the thermophysical properties in Eqs. (3) and (4), along with measured values for t_{Cu} and a. T_∞ and T_a are taken to be equal, T_{ss} is set for each data run, and t_{co} is measured when the test article cools to room temperature and the oxide film flakes off. These measurements

allow T_s to be determined (typically 1–3°C below T_{ss}), and, hence, $I_{\lambda b}(T_s)$ for λ as set by the monochromator can be calculated.

Uncertainty Analysis

Combining Eqs. (1) and (2), the uncertainty in the spectral–directional emittance may be stated

$$u_\varepsilon^2 = \left(\frac{\partial \varepsilon}{\partial R_e} u_{R_e}\right)^2 + \left(\frac{\partial \varepsilon}{\partial R_c} u_{R_c}\right)^2 + \left(\frac{\partial \varepsilon}{\partial T_c} u_{T_c}\right)^2 + \left(\frac{\partial \varepsilon}{\partial T_s} u_{T_s}\right)^2 \quad (5)$$

where $\delta\Omega$ and $\delta\lambda$ are considered to be perfectly repeatable (further low-order errors are considered in Ref. 16). Considering that as $T_c \approx T_s$, $I_{\lambda b}(T_c) \approx I_{\lambda b}(T_s)$, Eq. (5) may be reduced using Eqs. (1) and (2) to

$$u_\varepsilon^2 = (1 + \varepsilon^2)[t_{2,90}(S_{R_c}/R_c)]^2 + (4\varepsilon/T_s)^2(u_{T_c}^2 + u_{T_s}^2) \quad (6)$$

for three complete calibration spectra and a 90% confidence level. Taking the control tolerance for the uncertainty in the calibration temperature, and considering the effect of the terms in Eq. (3) on the surface temperature uncertainty, it may be shown that the emittance uncertainty is dominated by the radiometer reading uncertainty, and temperature uncertainty effects (including oxide layer thickness uncertainty) are insignificant. Hence, $u_\varepsilon \leq 0.06(1 + \varepsilon^2)^{1/2}$ for $T_s > 400$°C and 3 μm $\leq \lambda \leq 9$ μm, and $u_\varepsilon \leq 0.09(1 + \varepsilon^2)^{1/2}$ otherwise for the parameter ranges reported here.

Results

Reduced data showing the spectral–directional emittance of oxidized copper for surface temperatures of 399, 499, 598, and 697°C are given in Table 1. (Note that while the subsurface temperature was set at 400, 500, 600, and 700°C, the surface temperature is not known until the oxide thickness is measured.) Gaps in these data indicate measurements that could not be made repeatably because of low blackbody power. The normal emittance may be seen to increase with wavelength, increasing from ~0.6 at $\lambda = 2$ μm to ~0.9 at $\lambda = 10$ μm. At grazing angles this trend is more pronounced, with the emittance at $\theta = 84$ deg increasing from ~0.3 at $\lambda = 2$ μm to ~0.8 at $\lambda = 10$ μm. Emittances increase with temperature at all wavelengths and directions. There is a near linear increase in emittance between 399–697°C, at a rate that varies between about 0.3×10^{-3}/K at 4 μm and 0.2×10^{-3}/K at 8 μm. Naturally grown copper oxide is shown to be slightly directional at lower wavelengths and relatively diffuse at higher wavelengths. At $\lambda = 3.5$ μm, the emittance is relatively constant from the normal to $\theta = 48$ deg, and declines by about 30% between 48–84 deg (emittance at 90 deg cannot be measured with the present apparatus). However, at $\lambda = 9.5$ μm, emittance is diffuse to within 10% over the range from normal to grazing angles. Figure 3 is a polar plot of the measured spectral–directional emittance of fully oxidized copper at $\lambda =$ 3.5 and 9.5 μm for various temperatures.

The authors have been unable to locate any non-normal spectral–directional emittance data for copper oxide in the literature, with the exception of Burgess,[20] reported in 1909, where measurements for $\theta = 25$ deg are given for $\lambda = 0.55$ μm ($\varepsilon = 0.68$ and 0.49 for $T = 1100$ and 1200°C, respectively), and 0.65 μm ($\varepsilon = 0.80$, 0.60, and 0.49 for $T = 1000$, 1100, and 1200°C, respectively). Burgess' data cover a lower wavelength range and higher temperature range than the present data. Burgess' data suggest a decrease in emittance with increasing wavelength and a decrease in emittance with increasing temperature. Both trends are at odds with the present data. Many of the details of Burgess' work are inaccessible, making it difficult to comment in detail on its apparatus and procedure. However, Burgess' measurements continue to be cited in properties reference works.

Spectral–normal emittance data are presented by Coblentz[5] and Wieder,[13] and these are shown together with the present spectral–normal emittance in Fig. 4. Wieder (at 25°C) covers a spectral range beneath that of the present data, and comparison of the Wieder and the present data suggests that there is an emittance decrease with wavelength for low wavelengths, a minimum near 1 μm, and an increase at higher wavelengths. For quantitative comparisons, it must be cautioned that Wieder's data concern a copper oxide layer only 0.088 μm thick, whereas the oxide layer in the present data is 400 μm thick. Coblentz' data (reported in 1912, and also at 25°C) corresponds only very roughly with the present data.

The present data are integrated over polar angle to determine spectral–hemispherical emittance. Figure 5 shows spectra for different temperatures, demonstrating the increase with both wavelength and temperature. Note the anomalous points in Fig. 5 between 6–7 μm. These points are repeatable over three trials, but do not appear consistent with the other data. Since the optical path is open to ambient air and has a length of about 1.1 m, this behavior may be related to an air absorption band near 6.5 μm. However, the offset of these points with

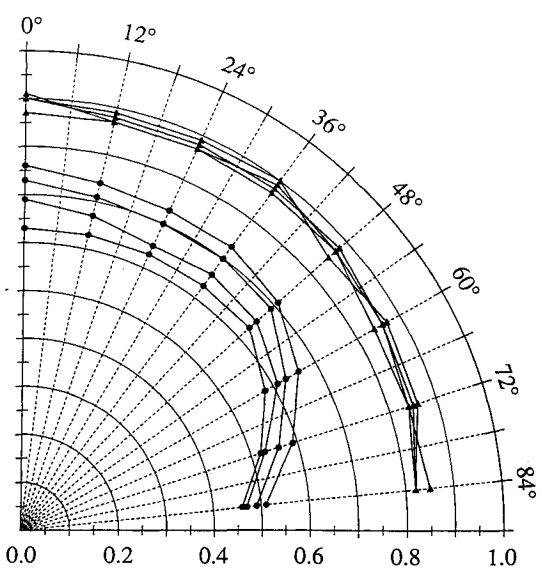

Fig. 3 Spectral–directional emittance of fully oxidized copper as a function of direction for wavelengths of 3.5 μm (-●-) and 9.5 μm (-▲-) and temperatures of 399°C (lower emittance), 499, 598, and 697°C (higher emittance).

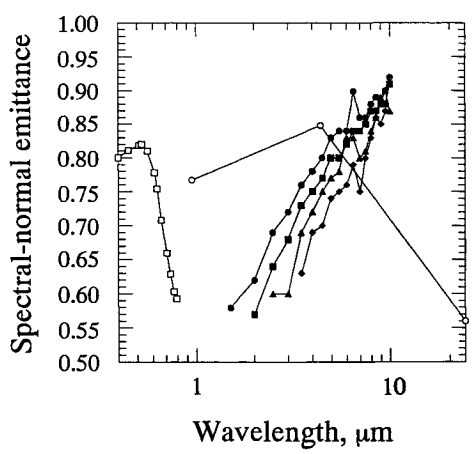

Fig. 4 Spectral–normal emittance of fully oxidized copper at various temperatures as a function of wavelength: 399°C (-◆-), 499°C (-▲-), 598°C (-■-), 697°C (-●-), Wieder[13] (-□-), and Coblentz[5] (-○-).

Table 1 Spectral–directional emittance of oxidized copper at 399°C (1st row), 499°C (2nd row), 598°C (3rd row), and 697°C (4th row)

	Polar angle, deg							
λ, μm	0	12	24	36	48	60	72	84
1.5	—	—	—	—	—	—	—	—
	—	—	—	—	—	—	—	—
	—	—	—	—	—	—	—	—
	0.58	0.58	0.58	0.58	0.54	0.49	0.40	—
2.0	—	—	—	—	—	—	—	—
	—	—	—	—	—	—	—	—
	0.57	0.57	0.57	0.57	0.52	0.48	0.38	—
	0.62	0.60	0.60	0.60	0.53	0.49	0.43	0.33
2.5	—	—	—	—	—	—	—	—
	0.60	0.60	0.60	0.60	0.60	0.54	0.42	—
	0.64	0.64	0.64	0.62	0.62	0.54	0.46	0.36
	0.69	0.68	0.67	0.65	0.63	0.58	0.50	0.41
3.0	—	—	—	—	—	—	—	—
	0.60	0.60	0.60	0.60	0.60	0.54	0.48	0.42
	0.68	0.68	0.68	0.68	0.65	0.59	0.50	0.44
	0.72	0.71	0.71	0.69	0.67	0.62	0.54	0.45
3.5	0.63	0.63	0.63	0.63	0.63	0.58	0.52	0.46
	0.69	0.67	0.65	0.66	0.65	0.61	0.53	0.47
	0.73	0.71	0.70	0.70	0.69	0.63	0.56	0.49
	0.76	0.74	0.73	0.73	0.71	0.66	0.59	0.51
4.0	0.69	0.69	0.69	0.69	0.69	0.63	0.56	0.50
	0.72	0.71	0.69	0.71	0.69	0.65	0.57	0.55
	0.75	0.73	0.72	0.73	0.72	0.68	0.62	0.56
	0.78	0.77	0.76	0.76	0.75	0.70	0.64	0.58
4.5	0.70	0.70	0.70	0.70	0.70	0.67	0.61	0.58
	0.75	0.73	0.71	0.73	0.73	0.70	0.63	0.60
	0.77	0.76	0.75	0.76	0.75	0.72	0.66	0.61
	0.80	0.78	0.78	0.78	0.76	0.74	0.68	0.62
5.0	0.74	0.74	0.74	0.74	0.74	0.70	0.66	0.62
	0.77	0.75	0.73	0.75	0.75	0.73	0.66	0.61
	0.80	0.77	0.77	0.79	0.79	0.74	0.70	0.65
	0.83	0.81	0.81	0.81	0.80	0.77	0.73	0.67
5.5	0.75	0.75	0.75	0.75	0.75	0.72	0.68	0.65
	0.78	0.76	0.76	0.76	0.76	0.74	0.70	0.66
	0.80	0.79	0.78	0.79	0.79	0.77	0.73	0.69
	0.84	0.82	0.82	0.82	0.82	0.80	0.76	0.72
6.0	0.76	0.76	0.76	0.76	0.76	0.73	0.73	0.70
	0.80	0.78	0.76	0.78	0.78	0.76	0.74	0.70
	0.82	0.80	0.80	0.80	0.80	0.78	0.76	0.72
	0.84	0.83	0.82	0.83	0.81	0.81	0.79	0.75
6.5	0.79	0.79	0.79	0.79	0.79	0.75	0.75	0.71
	0.83	0.81	0.81	0.81	0.81	0.81	0.76	0.73
	0.84	0.84	0.84	0.84	0.84	0.82	0.80	0.77
	0.89	0.87	0.86	0.86	0.86	0.86	0.83	0.79
7.0	0.75	0.75	0.75	0.75	0.78	0.75	0.75	0.72
	0.80	0.78	0.78	0.78	0.80	0.78	0.76	0.72
	0.84	0.81	0.81	0.83	0.81	0.80	0.78	0.75
	0.86	0.84	0.84	0.86	0.84	0.84	0.81	0.78
7.5	0.80	0.80	0.80	0.80	0.80	0.80	0.76	0.76
	0.81	0.81	0.79	0.81	0.81	0.81	0.79	0.74
	0.85	0.83	0.82	0.85	0.83	0.82	0.80	0.78
	0.86	0.84	0.84	0.86	0.84	0.83	0.82	0.79
8.0	0.83	0.83	0.83	0.83	0.83	0.83	0.78	0.78
	0.84	0.84	0.84	0.84	0.84	0.84	0.80	0.76
	0.87	0.85	0.85	0.85	0.85	0.85	0.82	0.79
	0.88	0.86	0.84	0.86	0.86	0.84	0.82	0.79
8.5	0.86	0.86	0.86	0.86	0.86	0.86	0.83	0.83
	0.86	0.86	0.87	0.84	0.86	0.87	0.83	0.80
	0.87	0.88	0.84	0.86	0.86	0.85	0.82	0.79
	0.89	0.85	0.85	0.87	0.90	0.87	0.83	0.80
9.0	0.85	0.85	0.85	0.85	0.85	0.85	0.86	0.83
	0.89	0.87	0.87	0.87	0.87	0.87	0.85	0.83
	0.88	0.85	0.87	0.87	0.85	0.87	0.82	0.83
	0.88	0.88	0.86	0.88	0.86	0.87	0.85	0.84
9.5	0.87	0.87	0.87	0.87	0.87	0.84	0.84	0.85
	0.90	0.88	0.88	0.88	0.88	0.86	0.84	0.82
	0.91	0.87	0.87	0.89	0.87	0.86	0.85	0.82
	0.90	0.89	0.89	0.90	0.85	0.87	0.86	0.82
10.0	—	—	—	—	—	—	—	—
	0.87	0.87	0.87	0.87	0.87	0.88	0.83	0.84
	0.91	0.89	0.89	0.87	0.87	0.86	0.83	0.84
	0.92	0.88	0.89	0.90	0.87	0.86	0.87	0.83

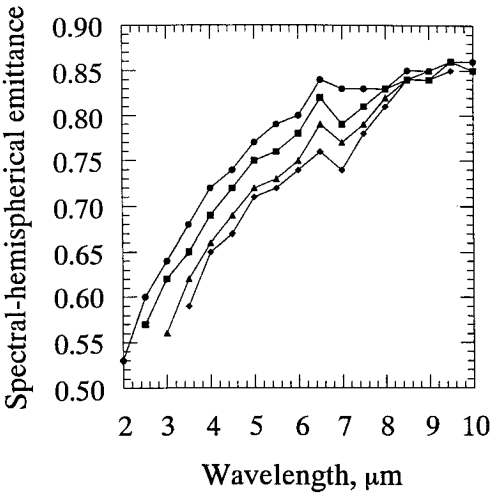

Fig. 5 Spectral–hemispherical emittance of fully oxidized copper as a function of wavelength: 399°C (-◆-), 499°C (-▲-), 598°C (-■-), and 697°C (-●-).

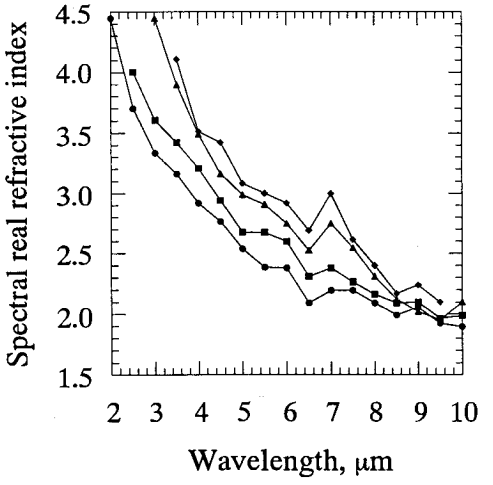

Fig. 6 Spectral real part of the index of refraction of copper oxide, reduced from rough surface data, as a function of wavelength: 399°C (-◆-), 499°C (-▲-), 598°C (-■-), and 697°C (-●-).

respect to the trend of the other data lies within the experimental uncertainty.

Considering the copper oxide film to be opaque and not electrically conducting, the spectral–directional emittance may be related to the real part of the index of refraction through the Fresnel relation:

$$\varepsilon_{\lambda,\theta}(T) = 1 - \frac{1}{2}\left\{\left[\frac{n_\lambda^2(T)\cos\theta - \sqrt{n_\lambda^2(T) - \sin^2\theta}}{n_\lambda^2(T)\cos\theta + \sqrt{n_\lambda^2(T) - \sin^2\theta}}\right]^2 + \left[\frac{\cos\theta - \sqrt{n_\lambda^2(T) - \sin^2\theta}}{\cos\theta + \sqrt{n_\lambda^2(T) - \sin^2\theta}}\right]^2\right\} \quad (7)$$

Equation (7) is compared to the present data, and $n_\lambda(T)$ is identified by minimizing the deviation. A standard deviation of 5% is found between Eq. (7) and the experimental data. (A two-parameter identification yields $k_\lambda \approx 0$, confirming the dielectric assumption). Figure 6 shows the spectra of fitted real part of the index of refraction for various temperatures. The index of refraction may be seen to decrease with both wavelength and temperature. Karlsson et al.[21] report the index of refraction for fully oxidized vacuum-deposited copper films at room temperature over the range from 0.3 to 1.5 μm, derived from normal reflection measurements. These data show a value of about $n_\lambda = 2.55$ and vanishing k_λ at 1.5 μm for both CuO and Cu_2O. This value is considerably lower than that derived from the present work for wavelengths in the 2–3 μm range, although the material configurations and temperatures differ significantly between Ref. 21 and the present work.

Conclusions

The spectral–directional emittance of oxidized copper is derived from measurements of the radiative intensity leaving the surface of an oxidized copper block. The oxide layer is naturally grown to its limiting thickness at elevated temperatures over long heating times, and is not dressed or polished in any way. Emittance data for this material show a strong increasing monotonic variation with a wavelength between 2–10 μm, and a moderate increasing monotonic variation with temperature between 400–700°C. An index of refraction reduced from emittance data for this dielectric material shows corresponding decreasing monotonic variation with wavelength and temperature. The material shows significant directional variation at lower wavelengths (on the order of 3.5 μm), and caution should be used in making a diffuse assumption. At longer wavelengths (on the order of 9.5 μm), directional variation is minimal, and a diffuse assumption is more valid. It is suggested that spectral–directional emittance determination by direct emission measurement, together with index of diffraction identification (if found to fit Fresnel or other relations), may be used to improve radiative surface property knowledge for other engineering materials as well as copper oxide.

Acknowledgments

Funding for this work was provided by the National Science Foundation, under Grant CTS-9209926, whose support is gratefully acknowledged. William F. Gale graciously provided his X-ray diffraction expertise to help identify the material. The authors wish to thank the reviewers of this article (conference and present version) for providing helpful suggestions.

References

[1]Gubareff, G. G., Janssen, J. E., and Torborg, R. H., *Thermal Radiation Properties Survey*, 2nd ed., Honeywell Research Center, Minneapolis, MN, 1960.

[2]Beobachter, H. F., *Mitteilungen der Kaiser Wilhelm Institut*, Eisenforsch, Dusselderfabhandl, Vol. 109, 1928, p. 225.

[3]Binkley, E. R., private communication, in the work cited in Ref. 1.

[4]Cammerer, J. S., "The Thermal Properties of Wood and Materials Containing Wood," *Holz als Rohund Wenkstoff*, Vol. 1, No. 6, 1938, pp. 206–213.

[5]Coblentz, W. W., "The Diffuse Reflecting Power of Various Substances," National Bureau of Standards Scientific Paper 196, 1912.

[6]Jacob, M., *Heat Transfer*, Vol. 1, Wiley, New York, 1949.

[7]King, W. J., *Handbook of Chemistry and Physics*, edited by C. D. Hodgman, 31st ed., Chemical Rubber Publishing, Cleveland, OH, 1949.

[8]Randolf, C. F., and Overhaltner, M. J., *Physics Review*, Vol. 1, 1913, p. 144.

[9]Roeser, W. F., and Wensel, H. T., *Handbook of Chemistry and Physics*, edited by C. D. Hodgman, 34th ed., Chemical Rubber Publishing, Cleveland, OH, 1952.

[10]Siegel, R., and Howell, J. R., "Thermal Radiation Heat Transfer," 3rd ed., Hemisphere, Washington, DC, 1992.

[11]Schmidt, E., and Eckert, E., "Uher die Richtungsverteilung der Wärmestrahlung von Oberflacken," *Forschung auf dem Gebeite des Ingenieurwes*, Vol. 6, 1935, pp. 175–183.

[12]Wade, W. R., "Measurement of Total Hemispherical Emissivity of Oxidized Metals at High Temperatures," NACA TN 4206, March 1958.

[13]Wieder, H., and Czanderna, A. W., "Optical Properties of Copper Oxide Films," *Journal of Applied Physics*, Vol. 37, No. 1, 1966, pp. 184–187.

[14]Heinisch, B., Quinto-Diez, P., and Sacadura, J. F., "Improvements in Spectral Directional Emissivity Measurement Techniques by Direct Methods," *Proceedings of the 7th International Heat Transfer Conference*, Vol. 4, Hemisphere, Washington, DC, 1982, pp. 509–513.

[15]Hesketh, P. J., Gebhart, B., and Zemel, J. N., "Measurements of the Spectral and Directional Emission from Microgrooved Silicon Surfaces," *Journal of Heat Transfer*, Vol. 110, No. 3, 1988, pp. 680–686.

[16]Brandenberg, W. M., and Clausen, O. W., "The Directional Spectral Emittance of Surfaces Between 200°C and 600°C," *Symposium on Thermal Radiation of Solids*, edited by S. Katzoff, NASA SP-55, 1965, pp. 313–319.

[17]Dorai-Raj, D. E., "Spectral-Directional Emittance of Fully Oxidized Copper," M.S. Thesis, Auburn University, Auburn, AL, 1995.

[18]Incropera, F. P., and DeWitt, D. P., *Fundamentals of Heat and Mass Transfer*, 3rd ed., Wiley, New York, 1990.

[19]Touloukian, Y. S., and DeWitt, D. P. (eds.), *Thermophysical Properties of Matter*, IFI/Plenum, New York, 1972.

[20]Burgess, G. K., "The Estimation of the Temperature of Copper by Means of Optical Pyrometers," *National Bureau of Standards Bulletin*, No. 6, 1909, pp. 111–119.

[21]Karlsson, B., Ribbing, C. G., Roos, A., Valkonen, E., and Karlsson, T., "Optical Properties of Some Metal Oxides in Solar Absorbers," *Physica Scripta*, Vol. 25, No. 6, 1982, pp. 826–831.